

Multi-material topology optimization for crack problems based on eXtended isogeometric analysis

Thanh T. Banh¹, Jaehong Lee¹, Joowon Kang² and Dongkyu Lee*¹

¹Department of Architectural Engineering, Sejong University, Seoul 05006, Korea

²Department of Architecture, Yeungnam University, Gyeongsan 38541, Korea

(Received March 27, 2020, Revised November 25, 2020, Accepted November 27, 2020)

Abstract. This paper proposes a novel topology optimization method generating multiple materials for external linear plane crack structures based on the combination of IsoGeometric Analysis (IGA) and eXtended Finite Element Method (X-FEM). A so-called eXtended IsoGeometric Analysis (X-IGA) is derived for a mechanical description of a strong discontinuity state's continuous boundaries through the inherited special properties of X-FEM. In X-IGA, control points and patches play the same role with nodes and sub-domains in the finite element method. While being similar to X-FEM, enrichment functions are added to finite element approximation without any mesh generation. The geometry of structures based on basic functions of Non-Uniform Rational B-Splines (NURBS) provides accurate and reliable results. Moreover, the basis function to define the geometry becomes a systematic p-refinement to control the field approximation order without altering the geometry or its parameterization. The accuracy of analytical solutions of X-IGA for the crack problem, which is superior to a conventional X-FEM, guarantees the reliability of the optimal multi-material retrofitting against external cracks through using topology optimization. Topology optimization is applied to the minimal compliance design of two-dimensional plane linear cracked structures retrofitted by multiple distinct materials to prevent the propagation of the present crack pattern. The alternating active-phase algorithm with optimality criteria-based algorithms is employed to update design variables of element densities. Numerical results under different lengths, positions, and angles of given cracks verify the proposed method's efficiency and feasibility in using X-IGA compared to a conventional X-FEM.

Keywords: multi-material; topology optimization; crack problem; X-IGA; IGA; X-FEM; Non-Uniform Rational B-spline

1. Introduction

Nowadays, structural material topology optimization problems are significant and demanding in many engineering fields as an innovative numerical and design approach for effectively finding the optimal structural layout under a reasonable material quantity. In detail, topology optimization has been widely used for designing mechanical components and other engineering applications such as macrostructures (Liu *et al.* 2016), heat dissipating device (Yi and Liu 2018), truss (Yang *et al.* 2018), cracked structure (Shobeiri 2015), plate-like structures (Banh and Lee 2019, Nguyen *et al.* 2018, Banh and Lee 2018b) and some other applications (Lee *et al.* 2010, Zuo *et al.* 2007, Doan and Lee 2019, Qiao *et al.* 2016). The pioneering study by Bendsoe and Kikuchi (1988) is to find an optimal material density distribution within a prescribed design domain. By using separate material phases, topology optimization is extended for multiple materials aiming to find the optimal structural layout under a given material most effectively. There have been a lot of researches exploiting and developing the advantages of multi-material

topology optimization such as a topology synthesis of multiple materials (Alonso *et al.* 2014), an alternating active-phase algorithm (Cottrell *et al.* 2009, Tavakoli and Mohsenind 2014), viscoelastically damped structures under time-dependent loading (Yun and Youn 2017), a generalized Cahn-Hilliard (C-H) model (Zhou and Wang 2007) and so on. To visualize the distribution of optimal multiple material densities, an alternating active-phase algorithm through the standard binary phase for topology optimization was presented by Tavakoli and Mohsenind (2014). Zhou and Wang granted a so-called phase-field method for topology optimization using multiple materials based on the Cahn-Hilliard (C-H) model (2006a, 2006b).

The previous studies usually considered structures with a continuous displacement field through the standard finite element method. This study treats the discontinuous displacement field created by given cracks via eXtended IsoGeometric Analysis to reduce the performance loss of discontinued models by using multiple materials. Essentially, structures are defined to get a continuous displacement field and are assumed not to include regions such as explicitly cracks. In other words, when a discontinuous displacement field such as crack problems is ignored, optimal topology results of the structure may lose design performance abilities due to substantially slight cracks or errors. It may be the cause of the insufficiency of structural performance in industrial applications.

*Corresponding author, Associate Professor
E-mail: dongkyulee@sejong.ac.kr

Isogeometric analysis (IGA) has bridged the geometric division between computer-aided design and the finite element method to analyze structures' behavior. Isogeometric analysis can present exactly complex geometric domains and satisfy the continuous condition of solution fields (Khatir and Abdek 2018, Khatir *et al.* 2017, 2019, 2019b, 2020). It makes IsoGeometric Analysis become a compelling method for simulating structures, especially for those related to high order differential equations. Due to the accuracy of analytical solutions of X-IGA is superior to a conventional X-FEM (Khatir and Abdek 2019), this method guarantees the reliability of the optimal multi-material retrofitting against external cracks through using topology optimization. The critical concept of IsoGeometric Analysis was first outlined by Hughes *et al.* (2005). With NURBS's primary advantages of eliminating the gap between computer-aided design and finite element analysis, an analysis model represents exact structural geometry. It is widely applied from engineering disciplines electromagnetics (Buffa *et al.* 2010), composite material (Nazargah 2014), fracture mechanics (Shojaee and Daneshmand 2015) to optimization fields (Qian 2013, Wall *et al.* 2008, Qian 2010). Inspired by the simulation of crack propagation problems without remeshing of eXtended Finite Element Method (X-FEM), Benson *et al.* (2010) discussed the combination of eXtended Finite Element Method and IsoGeometric Analysis as a potential capability of a generalized the finite element formulation. Nguyen and Bordas (2005) presented the IsoGeometric Analysis applied to Finite Element Method and related to computer implementation aspects. Moes *et al.* (2012) proposed a so-called eXtended IsoGeometric Analysis (X-IGA) to simulate of stationary and propagating cracks.

On a numerical simulation of topological problems optimized for cracked structures, Shobeiri (2015) presented a bi-directional evolutionary structural optimization method (BESO) for a single material. Topology optimization for cracked structures using multiple materials and an eXtended Finite Element Method was proposed by Banh and Lee (2018a). The present study also deals with a numerical solution to distributing multiple material densities in a given cracked structure. However, efficient mechanical descriptions of material discontinuous boundaries are produced using an eXtended IsoGeometric Analysis, i.e., an interaction of IGA and X-FEM. In this approach, basic functions of Non-Uniform Rational B-Splines play the same role as shape functions of Finite Element Method for the geometrical crack description of structures. At the same time, control points and patches are dealt with as nodes and elements, respectively. Besides, optimal topology changes conforming to various crack information are also investigated to show the suggested approach's efficiency and feasibility.

This study contributes to as follows: (1) The accuracy of analytical solutions of X-IGA over the crack problem, which is superior to the conventional X-FEM, guarantees the reliability of the optimal multi-material distribution retrofitting against cracks through using topology optimization, and (2) The use of different multi-materials within a given external cracked structure produces the best

solution of structural performance, such as stiffness resulting from the present topology optimization method based on eXtended IsoGeometric Analysis. Thanks to the contributions as mentioned above, in the near future, this study makes toward 3-dimensional models with constrained parameters to gain the optimal computer-aided design before uploading on, especially, a 3-dimensional printing system.

The remainder of this study is organized as follows. Section 2 introduces a brief on several fundamental components and the methodology of constructing a discrete approximation to the displacements of X-IGA for linear elastostatic structures. In detail, multi-material densities in a patch using X-IGA, optimization models, compliance formulation, and sensitivity analysis are described in Section 3. The computational procedures of the present method are described in Section 4. Numerical examples of the present method are investigated and discussed in Section 5, including comparisons of analytical solutions X-IGA and X-FEM. And the conclusions are drawn in Section 6.

2. Formulations of eXtended IsoGeometric Analysis (X-IGA) for crack structures

In this section, some fundamental concepts of eXtended IsoGeometric Analysis and its implementation for external plane linear crack problems are presented. More details could be found in Moes *et al.* (1999), Nguyen and Bordas (2005), and Ghorashi *et al.* (2012).

2.1 Fundamental formulations of NURBS

NURBS is one of generalization of B-splines which in turn are piecewise polynomial curves composed by the B-spline basis functions. A knot vector $\Xi = \{\xi_1, \xi_2, \dots, \xi_{n+p+1}\}$ is defined as a non-decreasing sequence of parameter value $\xi_i \in \mathbb{R}$, where ξ_i is called i -th knot in the parametric space; p and n are the order and the number of basic functions, respectively. The univariate B-spline basis functions $N_{i,p}(\xi)$ are defined by the Cox-De Boor recursion formula (Cottrell *et al.* 2009) on the corresponding knot vector given by as follows

$$N_{i,0} = \begin{cases} 1 & \text{if } \xi_i \leq \xi \leq \xi_{i+1} \\ 0 & \text{otherwise} \end{cases} \quad (1)$$

For $p \geq 1$ its definition is written as

$$N_{i,p}(\xi) = \frac{\xi - \xi_i}{\xi_{i+p} - \xi_i} N_{i,p-1}(\xi) + \frac{\xi_{i+p+1} - \xi}{\xi_{i+p+1} - \xi_{i+1}} N_{i+1,p-1}(\xi) \quad (2)$$

Derivatives of the B-spline basis function can be formulated as

$$\frac{dN_{i,p}}{d\xi}(\xi) = \frac{p}{\xi_{i+p} - \xi_i} N_{i,p-1}(\xi) - \frac{p}{\xi_{i+p+1} - \xi_{i+1}} N_{i+1,p-1}(\xi) \quad (3)$$

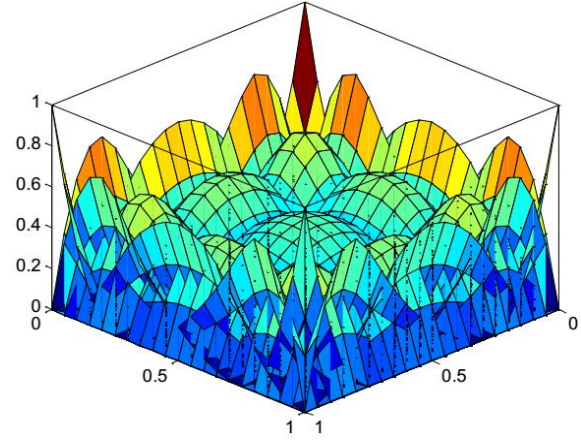
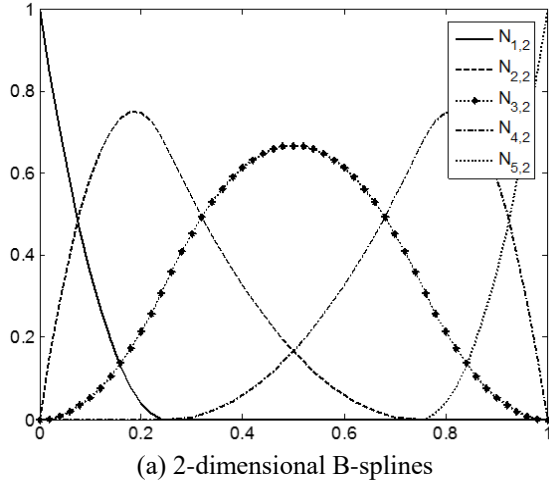


Fig. 1 B-spline basis functions within one and two dimensions

Fig. 1 describes an example of a B-spline function with knot vector $\Xi = \{0, 0, 0, 0.25, 0.75, 1, 1, 1\}$. Based on two parametric dimensions ξ and λ associated with two-knot vectors $\Xi = \{\xi_1, \xi_2, \dots, \xi_{n+p+1}\}$ and $\Lambda = \{\lambda_1, \lambda_2, \dots, \lambda_{m+q+1}\}$, the B-spline surface can be written as

$$\mathbf{S}(\xi, \lambda) = \sum_{i=1}^n \sum_{j=1}^m N_{i,p}(\xi) M_{j,q}(\lambda) \mathbf{P}_{i,j} = \sum_{I=1}^{n \times m} N_I^B(\xi, \lambda) \mathbf{P}_I \quad (4)$$

where $N_{i,p}(\xi)$ and $M_{j,q}(\lambda)$ are univariate B-spline basis functions; $N_I^B(\xi, \lambda)$ is B-spline shape function associated with the node $I = i(p+1) + j$; \mathbf{P} is a bidirectional control net.

To more accurately describe complex geometries or arbitrary shapes, a new parameter $w_{i,j}^s$ is added, which denotes an individual weight to control the geometric boundary. Finally, NURBS basis functions for a NURBS surface can be expressed as

$$\mathbf{S}(\xi, \lambda) = \sum_{i=1}^n \sum_{j=1}^m R_{i,j}^{p,q} \mathbf{P}_{i,j} = \sum_{I=1}^{n \times m} R_I(\xi, \lambda) \mathbf{P}_I \quad (5)$$

with

$$R_{i,j}^{p,q} = \frac{N_i^p(\xi) M_j^q(\lambda) w_{i,j}^s}{\sum_{i=1}^n \sum_{j=1}^m N_i^p(\xi) M_j^q(\lambda) w_{i,j}^s}, \quad R_I(\xi, \lambda) = \frac{N_I^B w_I^B}{\sum_{k=1}^{m \times n} N_k^B w_k^B} \quad (6)$$

2.2 Formulations of eXtended Isogeometric Analysis

In eXtended IsoGeometric Analysis, the displacement field approximation up at $\mathbf{x} = (X_1, X_2)$ can be presented as

$$u^p(\mathbf{x}) = \sum_{I \in \mathcal{N}} R_I(\xi, \lambda) \mathbf{u}_I + \sum_{J \in \mathcal{S}_I} R_J(\xi, \lambda) H(\xi, \lambda) \mathbf{a}_J + \sum_{K \in \mathcal{S}_I} R_K(\xi, \lambda) \sum_{\alpha=1}^4 \psi^{(\alpha)} b_K^{(\alpha)} \quad (7)$$

Sets of enrichment elements around cracks are called enriched tip node \mathcal{S}^T and step enriched nodes \mathcal{S}^L . \mathbf{u}_I denotes the DOFs vector at the I -th control point of standard Finite Element Method. \mathbf{a}_J and \mathbf{b}_K are enrichment DOFs vector parts as shown in Fig. 2.

H denotes Heaviside function which has role as a discontinuous function

$$H(\mathbf{x}) = \begin{cases} 1 & \text{for } (\mathbf{x} - \mathbf{x}^*) \cdot \mathbf{e}_n > 0 \\ -1 & \text{for } (\mathbf{x} - \mathbf{x}^*) \cdot \mathbf{e}_n < 0 \end{cases} \quad (8)$$

where \mathbf{x}^* is a given point. Figure 3 illustrates an example of the enrichment function for the elements cut by the crack with $\Xi = \{0, 0, 0, 1/3, 2/3, 1, 1, 1\}$.

Asymptotic crack tip function $\psi^\beta(r, \theta)$ with $\beta = \overline{1, 4}$ is used as enrichment functions to improve the accuracy of the solution by enhancing the description of singular fields close to the crack tip

$$\{\psi^\beta(r, \theta)\}_{\beta=1}^4 = \left\{ \sqrt{r} \sin \frac{\theta}{2}, \sqrt{r} \cos \frac{\theta}{2}, \sqrt{r} \sin \phi \sin \frac{\theta}{2}, \sqrt{r} \sin \phi \sin \frac{\theta}{2} \right\} \quad (9)$$

with r and θ which are local polar coordinates in physical space as follows

$$\begin{cases} r = \sqrt{x_1^2 + x_2^2} \\ \theta = \arctan(x_2 / x_1) \end{cases} \quad (10)$$

where (x_1, x_2) is local coordinates at the crack tip $\mathbf{x} = (x_{1T}, x_{2T})$

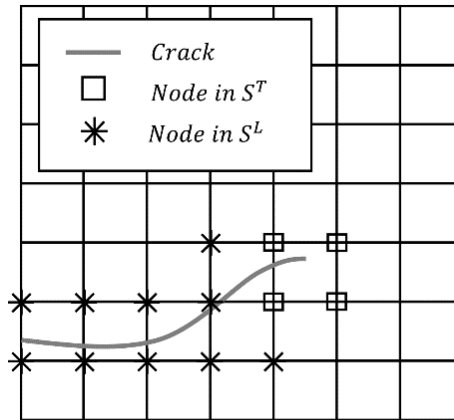


Fig. 2 Enrichment control point nodes of a given crack model

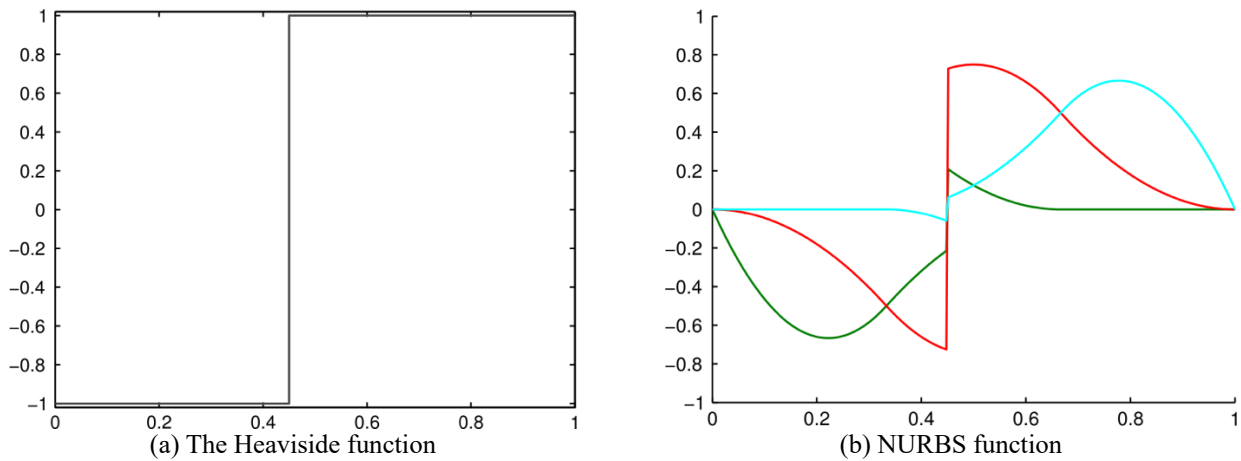


Fig. 3 An example illustrates the enrichment function for the elements cut by the crack

$$\begin{Bmatrix} x_1 \\ x_2 \end{Bmatrix} = \begin{bmatrix} \cos \phi & \sin \phi \\ -\sin \phi & \cos \phi \end{bmatrix} \begin{Bmatrix} X_1 - X_{1T} \\ X_2 - X_{2T} \end{Bmatrix} \quad (11)$$

where ϕ is the crack inclination angle with respect to the horizontal line at the tip and the following physical coordinates \mathbf{X} for a typically point in the parametric coordinate.

$$\mathbf{X}(\xi, \lambda) = \sum_{i=1}^N N_i(\xi, \lambda) \mathbf{P}_i \quad (12)$$

In this study, a so-called sub-triangle technique from X-FEM is generated to overcome the reduction of integration accuracy, as shown in Fig. 4, whose boundaries match the external plane crack's shape. Accordingly, in each element loop of a weak form, integration cut by cracks is replaced by sub-triangles.

3. Multi-material topology optimization formulations for crack problems materials based on X-IGA

Fig. 5 shows a typical design domain-schema of topology optimization problem by using multiple materials, where Ω_s^m and Ω_v^m represent solid and void materials, respectively. Being similar to standard Finite Element Method, the entire domain is discretized into patches. According to Bendsøe and Sigmund (1990), void material is also considered the same role of a separate material phase. Therefore, modified SIMP version of linear interpolation for multi-material is expressed by

$$E(\gamma) = \sum_{i=1}^{n+1} \gamma_i^p E_i^0 \quad (13)$$

where γ and p denote design variables and a penalization factor, respectively. E_i^0 is Young's modulus corresponding to material phase γ_i and $\sum_i \gamma_i = 1$. By using alternating active phase algorithm in conjunction with the block Gauss-Seidel method, a multiphase topology optimization problem with multiple volume fraction constraints is generated. Moreover, only two phases 'a' and 'b' are activated in each sub-process, the remaining phases

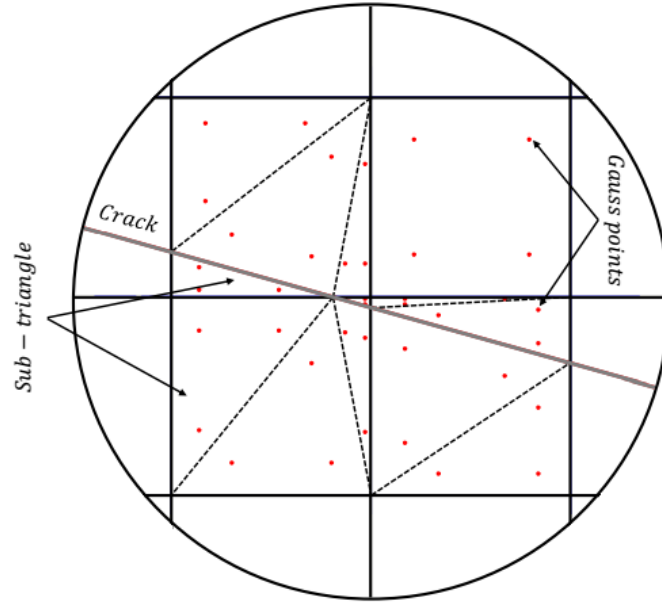


Fig.4 Sub-elements and Gauss points is re-selected by the influence of crack

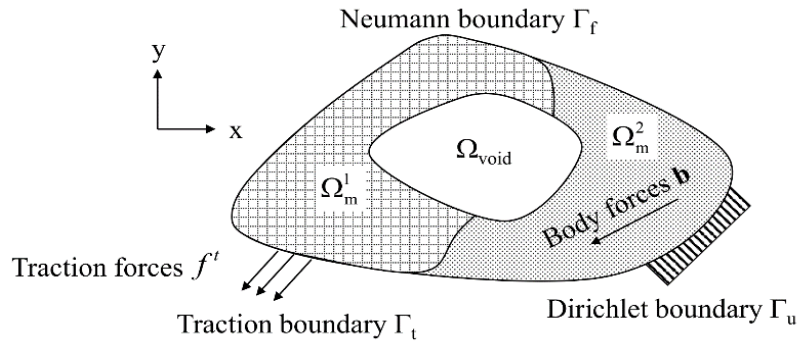


Fig. 5 Typical design domain schema of topology optimization by using multiple materials

are fixed. Note that the density of active phase ‘a’ in each binary phase topology optimization subproblem acts as the only design variable. Finally, the density of phase ‘b’ can be easily calculated through the density of corresponding phase ‘a’ by the density summation formulation of two active phases at each point $x \in \Omega$

$$\gamma_a(x) + \gamma_b(X) = 1 - \sum_{i=1, i \neq \{a,b\}}^{n+1} \gamma_i(X) \quad (14)$$

3.1 Topology optimization model by using multiple materials

By using NURBS basis function of Eq. (5) for a patch p , the displacement function $\mathbf{u}^p = [u, v]$ can be expressed as

$$\mathbf{u}^p(\xi, \lambda) = [u(\xi, \lambda), v(\xi, \lambda)] = \sum_{i=1}^n \sum_{j=1}^m R_{i,j}^{p,q} \mathbf{U}_{i,j} = \mathbf{R}\mathbf{U}^p \quad (15)$$

where $R_{k,l}(\xi, \lambda)$ is the rational term with $(\xi, \lambda) \in [\xi_i, \xi_{i+1}] \times [\lambda_j, \lambda_{j+1}]$.

The general compliance formulation C in structural topology optimization problem by using multiple materials can be mathematically stated as

$$\begin{aligned} &\underset{\gamma_i}{\text{minimize:}} && C(\gamma_i, \mathbf{U}) = \mathbf{U}^T \mathbf{K}(\gamma_i) \mathbf{U} \\ &&& \mathbf{K}(\gamma_i) \mathbf{U} = \mathbf{F} \\ &\text{subject to:} && \int_{\Omega} \gamma_i d\Omega \leq V_i \\ &&& 0 < \varepsilon_i \leq \gamma_i \leq 1 \end{aligned} \quad (16)$$

where V_i is a volume fraction in each material with $i = \overline{1:n+1}$, here $\sum_i V_i = 1$. \mathbf{U} is a global control point displacement by cracks. \mathbf{F} is a global load vector, and a global stiffness matrix is denoted by \mathbf{K} .

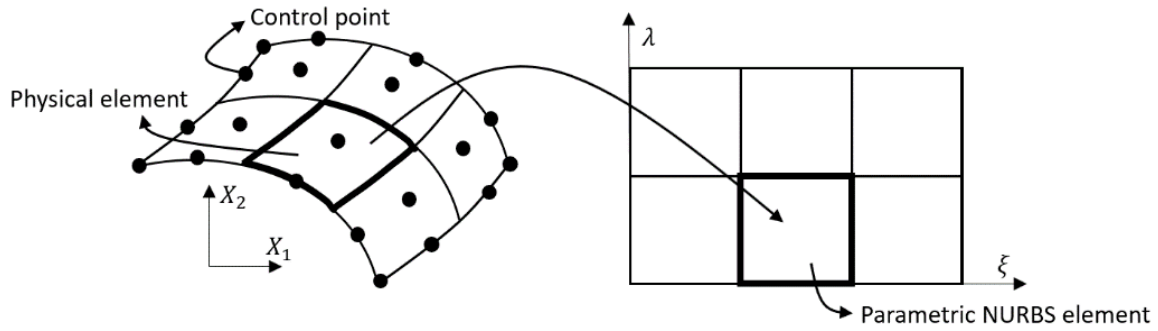


Fig. 6 Diagrammatic interpretation of mappings from a parametric to a physical space

3.2 Stiffness and sensitivity formulation by using X-IGA

According to Eqs. (7) and (13) into Eq. (16), by using a standard Galerkin method procedure, stiffness matrix of cracked structures for a single patch is formulated as follows.

$$\mathbf{K} = \iint_{\Omega} \mathbf{B}^T(\xi, \lambda) \left(\sum_{k=1}^{n+1} \gamma_k^p \mathbf{D}_k^0 \right) \mathbf{B}(\xi, \lambda) |\mathbf{J}| \bar{t} d\xi d\lambda \quad (17)$$

where \bar{t} is thickness. \mathbf{D}_k^0 is material property matrix corresponding to phase k -th including Poisson's ratio ν and nominal elastic modulus E .

$$\mathbf{D}_k^0 = \frac{E_k^0}{1-\nu^2} \begin{bmatrix} 1 & \nu & 0 \\ \nu & 1 & 0 \\ 0 & 0 & (1-\nu)/2 \end{bmatrix} \quad (18)$$

\mathbf{J} is Jacobian matrix describing the relationship between physical coordinate system and NURBS parameter space as shown in Fig. 6

$$\mathbf{J} = \begin{bmatrix} \sum_I^{n \times m} R_{I,\xi} P_{X_1} & \sum_I^{n \times m} R_{I,\lambda} P_{X_1} \\ \sum_I^{n \times m} R_{I,\xi} P_{X_2} & \sum_I^{n \times m} R_{I,\lambda} P_{X_2} \end{bmatrix} \quad (19)$$

in which P_{X_1} and P_{X_2} are compositions of control nets.

The deformation of matrix \mathbf{B} can be written as follows.

$$\mathbf{B} = \begin{bmatrix} \sum_I^{n \times m} R_{I,\xi} P_{X_1} & \sum_I^{n \times m} R_{I,\lambda} P_{X_1} \\ \sum_I^{n \times m} R_{I,\xi} P_{X_2} & \sum_I^{n \times m} R_{I,\lambda} P_{X_2} \end{bmatrix} \quad (20)$$

with

$$\mathbf{B}^{std} = \begin{bmatrix} R_{I,X_1} & 0 \\ 0 & R_{I,X_2} \\ R_{I,X_2} & R_{I,X_1} \end{bmatrix} \quad (21a)$$

$$\mathbf{B}^{enr} = \begin{bmatrix} R_{I,X_1} \Upsilon_I + R_I \Upsilon_{I,X_1} & 0 \\ 0 & R_{I,X_2} \Upsilon_I + R_I \Upsilon_{I,X_2} \\ R_{I,X_2} \Upsilon_I + R_I \Upsilon_{I,X_2} & R_{I,X_1} \Upsilon_I + R_I \Upsilon_{I,X_1} \end{bmatrix} \quad (21b)$$

where \mathbf{B}^{std} and \mathbf{B}^{enr} denote a standard strain-displacement and enriched parts of matrix \mathbf{B} , respectively. Υ_I represents Heaviside function ($\Upsilon_I = H$) and asymptotic basis functions ($\Upsilon_I = \psi^\beta$).

In each patch, a local volume fraction is assumed to have a unit volume $\partial V / \partial \gamma_a^p = 1$. By differentiating Eq. (14), sensitivities of compliance C for topology optimization in terms of multiple materials can be expressed

$$\frac{\partial C}{\partial \gamma_a^p} = -(\mathbf{U}^p)^T \frac{\partial \mathbf{K}^p}{\partial \gamma_a^p} \mathbf{U}^p \quad (22)$$

where γ_a^p and \mathbf{U}^p are a density of phase 'a' and an element displacement vector of patch p -th, respectively. Derivative of elemental stiffness in terms of design variable 'a' is written as

$$\frac{\partial \mathbf{K}_{IJ}^{rs}}{\partial \gamma_a^p} = p \gamma_a^{p-1} \int_{\Omega^p} (\mathbf{B}_I^r)^T (\mathbf{D}_a^0 - \mathbf{D}_b^0) \mathbf{B}_J^s d\Omega \quad (23)$$

where $r, s = \mathbf{u}, \mathbf{a}, \mathbf{b}$.

Finally, the filtered sensitivity of compliance $\partial C / \partial \gamma_a^p$ with respect to density of phase 'a' can be derived as

$$\frac{\partial \bar{C}}{\partial \gamma_a^p} = \frac{\sum_i H_{ei} \gamma_{ai}^e \frac{\partial C}{\partial \gamma_a^p}}{\gamma_a^p \sum_i H_{ei}} \quad (24)$$

where the convolution operator H is based on the distance to neighborhood elements as

$$H_{ei} = r_{\min} - \text{dist}(e, \{f \in N \mid \text{dist}(e, f) \leq r_{\min}\})$$

Furthermore, $\text{dist}(e, f)$ is the distance between the center of element e and f . The neighborhood elements are

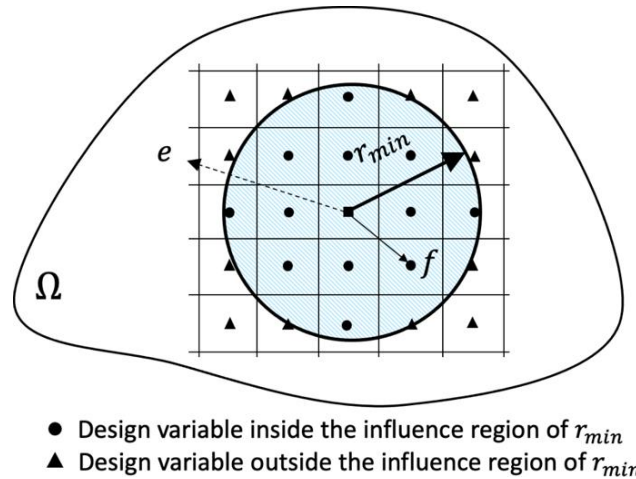


Fig. 7 Relationship between parameters in the convolution operator H_{ei} .

defined within a circle with the filter radius r_{min} as shown in Fig 7.

4. Computational procedure algorithm of the present method

Topology optimization produces optimal material distribution in a given design domain under constraints so that the optimal design offers the best structural performance for a given physical cracked problem. In this section, a briefly summarized algorithm of the present method using the combination of X-FEM and IGA, i.e., X-IGA as an analysis model, is described in Fig. 8.

A suitable reference domain with given loading directions, fixed boundary conditions, and a finite element mesh is determined in advance as an initialization step to perform eXtended IsoGeometric Analysis steps. From Eqs (17) to (22), the sensitivity of compliance regarding multi-material design variables is calculated. And then, the sensitivity filtering is applied to avoid the checkerboard phenomena. Finally, multi-material design variables are re-updated through these continuous iterative processes until arriving at the desired optimal convergence.

5. Numerical examples and discussion

First, an accurate modeling benchmark test for a specific edge crack in a finite tensile plate is executed and compared to assess the present method's performance. To verify the proposed method's accuracy, numerical results are compared with results obtained by the typical eXtended Finite Element Method. Domain-based interaction integral is used to obtain the individual SIFs-application of path independent integral to derive the SIFs results in a sufficiently accurate technique. The evaluation of SIFs by domain-based integration integral uses only those field variables, not in the crack tip close vicinity. This interaction integral proves beneficial while obtaining the individual

SIFs from a solution only if the auxiliary field is judiciously chosen. In this example, the normalized stress intensity factor (SIF) can be defined as $\bar{K}_I = K_I / (\sigma\sqrt{\pi a})$

(Mohammadi 2008). Fig. 9 shows the verification of eXtended IsoGeometric Analysis 's accuracy and superiority compared with the conventional eXtended Finite Element Method in cracked structure analysis. As can be seen, the analytical value of eXtended IsoGeometric Analysis using a second basis function (rather than that of the first-order low function) is more accurate with better convergence in comparisons with X-FEM. By using p-refinement, eXtended IsoGeometric Analysis can achieve high accuracy with even coarse meshes by controlling the field approximation order. In general, this method allows for analyzing the structure and provides a significant reduction in computational cost.

Next, three examples of topologically optimizing a cantilever beam structure of a plain stress state with multi-material and initial external cracks are considered, as shown in Figs. 10, 15, and 19. A design domain in which an assumed crack such as a natural crack in practice is allocated is given, and it is a non-dimensional rectangular space with $L \times H = 30 \times 10$. The left side of the domain is fixed, and the downward force with non-dimensional magnitude $F = 200$ is applied at the bottom point of the free end. The penalization factor, radius filter r_{min} and Poisson's ratio for variable materials are fixed to be 3.0, 8.0 and 0.3, respectively. In this study's scope, first-order basis functions along with 49×17 control points are used to approximate displacement fields. The mesh of 51×19 patches and the weight value $\{w_i\} = 1$ are used in all examples. The optimal results are investigated for cases of single and two materials. Properties of all materials are shown in Table 1. Here, Young's modulus and volume fraction of void material are $E_v = 10^2$ and $V_v = 1 - \sum_{k, k \neq v} V_k$, respectively, for all examples.

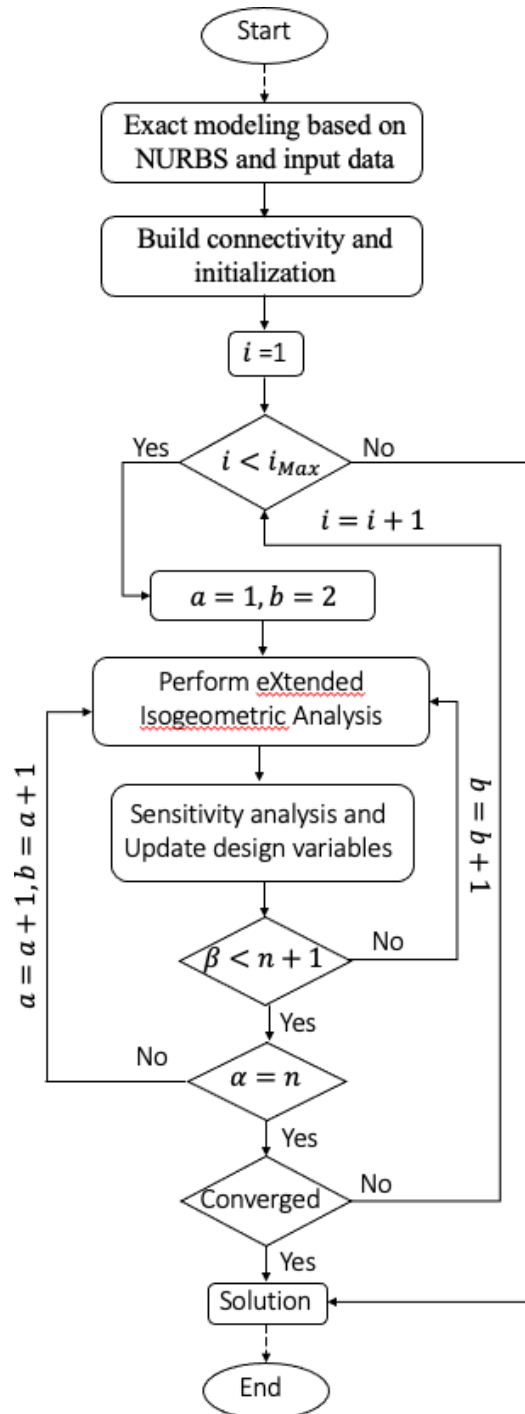


Fig. 8 Flowchart of extended isogeometric based topology optimization for crack structures by using multiple materials

5.1 Optimal topology generation results under a mechanical description of Initial crack's length

Two lengths of each crack l_c of 2.125 and 4.125 are considered, as shown in Fig. 10. During every optimization iteration for all examples, the volume fraction is controlled to be 40% of the initial total volume.

Figs. 11 and 12 describe optimal topologies for single material and two materials using X-IGA and X-FEM,

respectively. As can be seen, the length of one crack significantly affects optimal topology and shape distributions varying material densities within the design domain. Stresses within the design domain tend to increase close a tip crack, load and supported area. Therefore, material density distribution also tends to concentrate around the tip crack to hold structure stability. The results of X-IGA are mostly similar to those by X-FEM concerning optimal topology, even though converged compliance values are somewhat different. According to Fig. 9, Optimal

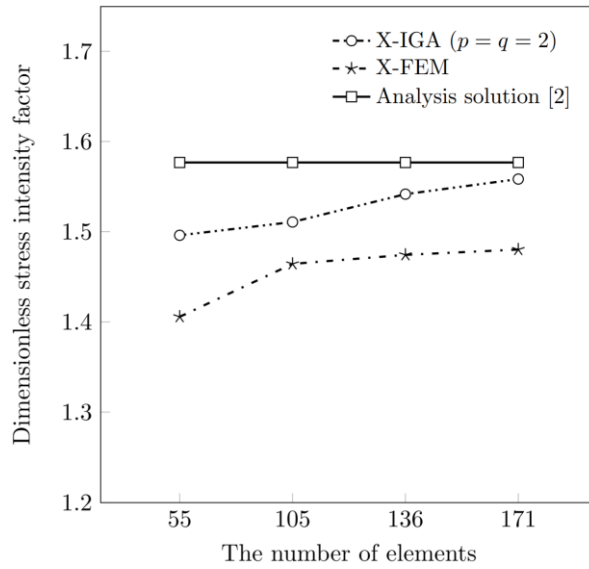


Fig. 9 Accurate modeling results of normalized stress intensity factor with $a/L = 0.275$

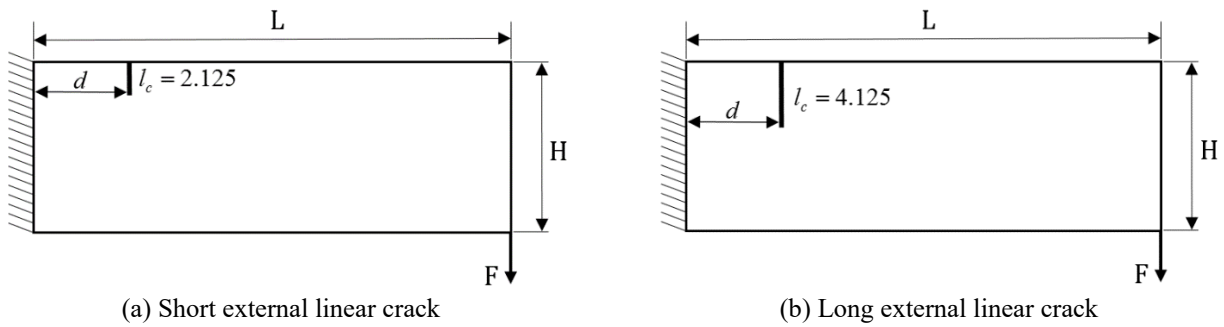


Fig. 10 Problem definition evaluating the influence of one crack length in a given design domain

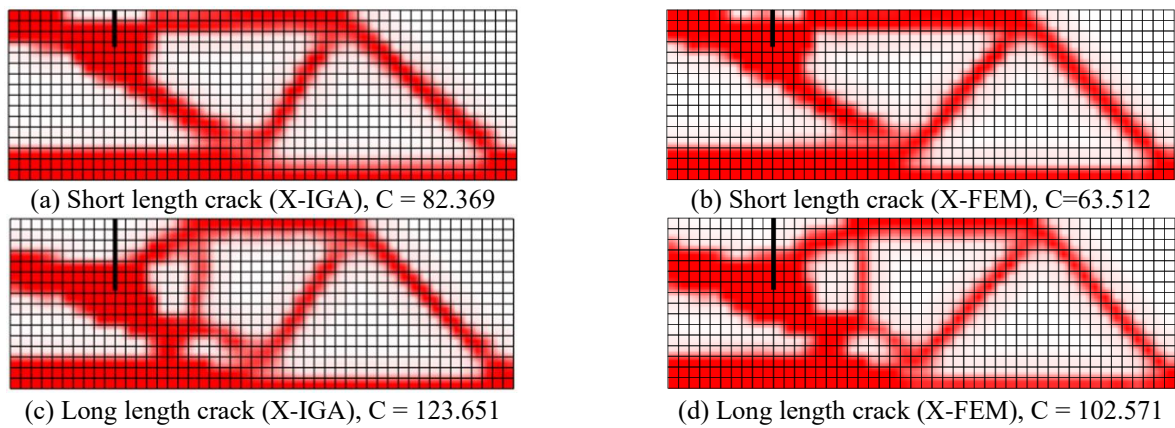


Fig. 11 Optimal single material topologies

Table 1 Caption

| Material properties | Number of materials | |
|---------------------|---------------------|--------------------------------|
| | (a) One (red) | (b) Teo (red, blue) |
| Young's modulus | $E_r^0 = 200e3$ | $E_r^0 = 200e3, E_b^0 = 400e3$ |
| Poisson's ratio | $\nu = 0.3$ | |
| Volume fraction | $V_r = 40\%$ | $V_r = 15\%, V_b = 25\%$ |

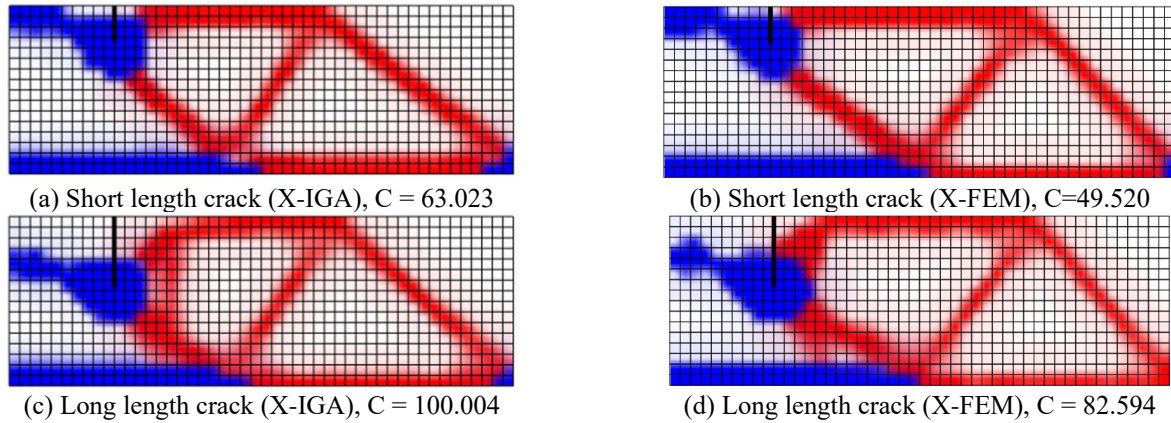


Fig. 12 Optimal two-materials topologies

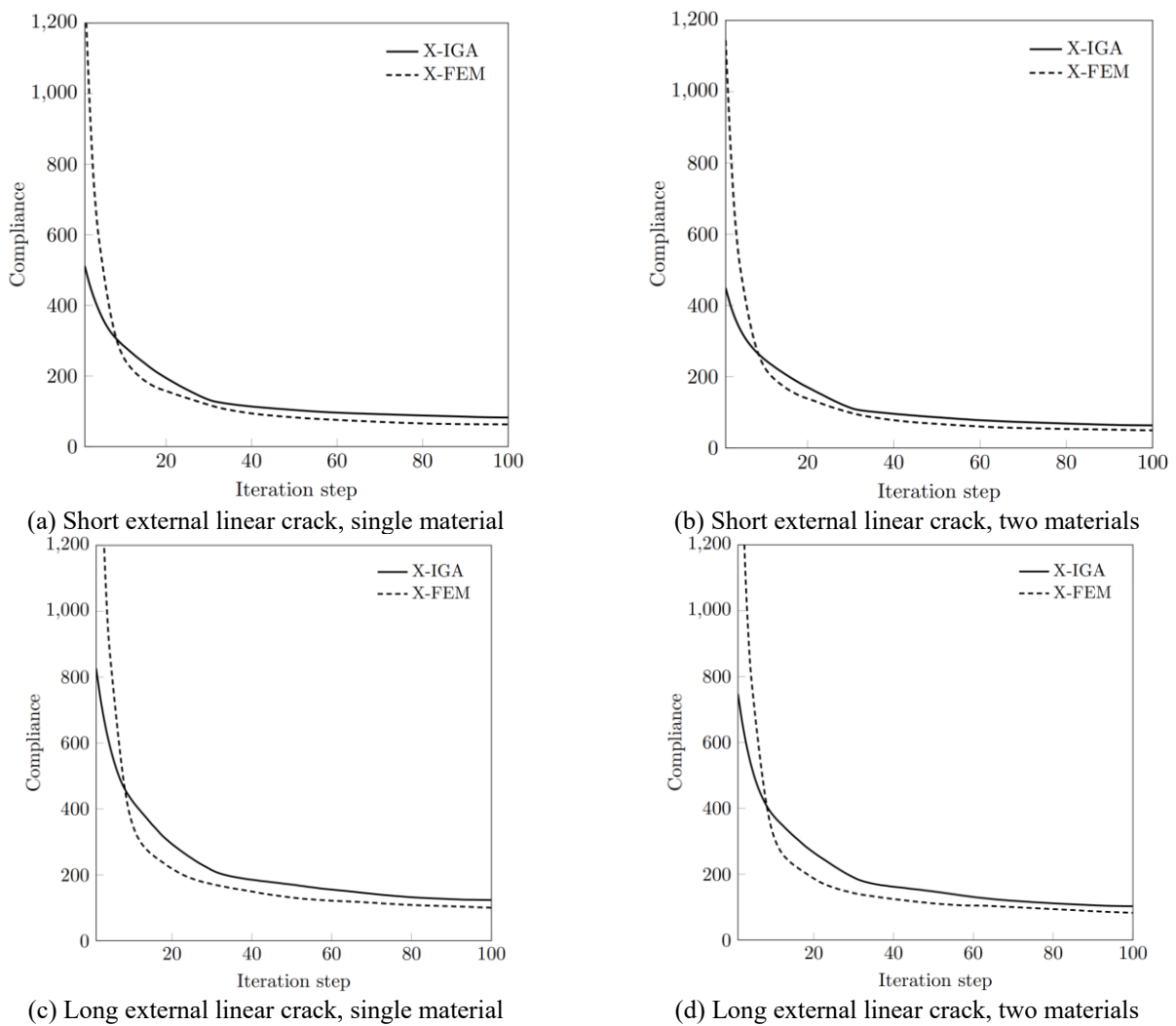


Fig. 13 Convergence histories of objective functions dealing with X-IGA and X-FEM in example 1

results of X-IGA may be more reliable and exact than those of X-FEM in case of crack problems. It demonstrates the numerical stability of X-IGA concerning topologies optimized with multiple materials.

Fig. 13 shows convergence histories of objective functions relying on crack's length with 40% of initial volume. In this result, longer cracked structure results in less stiff converged compliance.

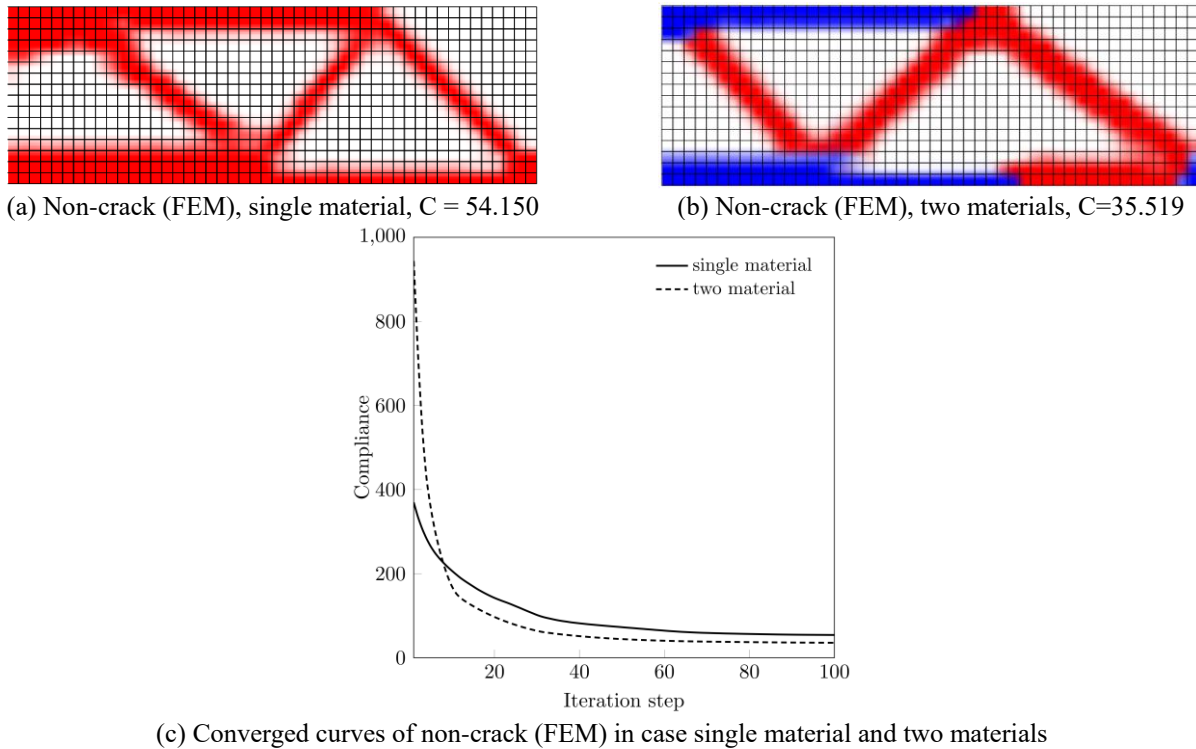


Fig. 14 Optimal results of single material and two materials in case non-crack finite element method

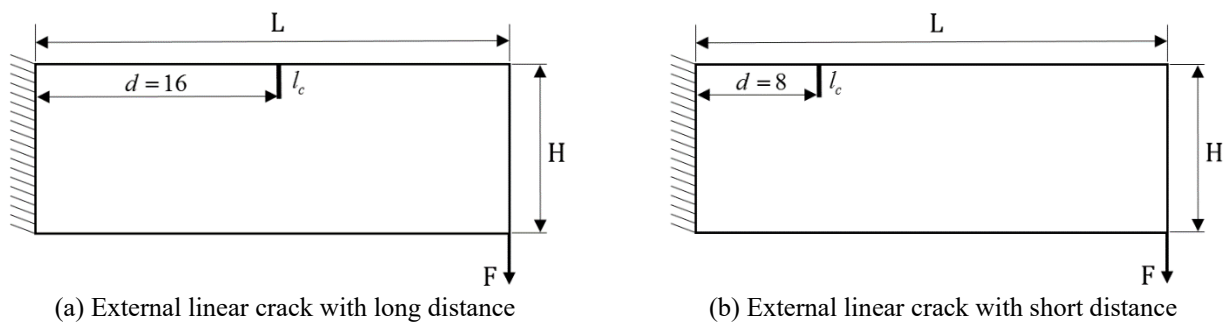


Fig. 15 Problem definition evaluating the influence of one crack location in a given design domain

For the purpose of comparing with previous example 1 results, Fig. 14 describes optimal topologies and converged curves in the typical case of non-crack structures for single material and two materials.

5.2 Optimal topology generation results under a mechanical description of Initial crack's location

For the purpose of the effect of crack's location, two location cases of one initial crack are considered, such as $d = 16$ and $d = 8$ with the same crack length $l = 2.125$ as shown in Fig. 15.

Figs. 16 and 17 show optimized topologies considering single material and two materials in different crack locations. Material density distributions are focused near the given crack area to retrofit stiffness reduction due to stress concentration occurred by load effects.

Fig. 18 shows convergence histories of objective function depending on one crack's location under a given volume fraction of 40%. As can be seen, converged compliance values of the crack's location close to fixed boundaries are more extensive than those far from fixed boundaries. Moreover, the long distance of one crack results in less stiff converged compliance due to boundary conditions in both single and two material cases. As shown in Figs 11, 12, and 16, 17, it is common to be confused about compliance accuracy. As figured out in Fig. 9, both the conventional X-FEM and the X-IGA provide displacement results below the exact solution in elastic problems. By using the same analysis mesh, higher-order elements produce larger displacement results than those of lower-order ones. Due to strain energy formulation, $C = (1/2)\mathbf{U}^T \mathbf{K} \mathbf{U} = (1/2)\mathbf{U}^T \mathbf{F}$, the displacement vector \mathbf{U} is dependent on discretization meshes and element

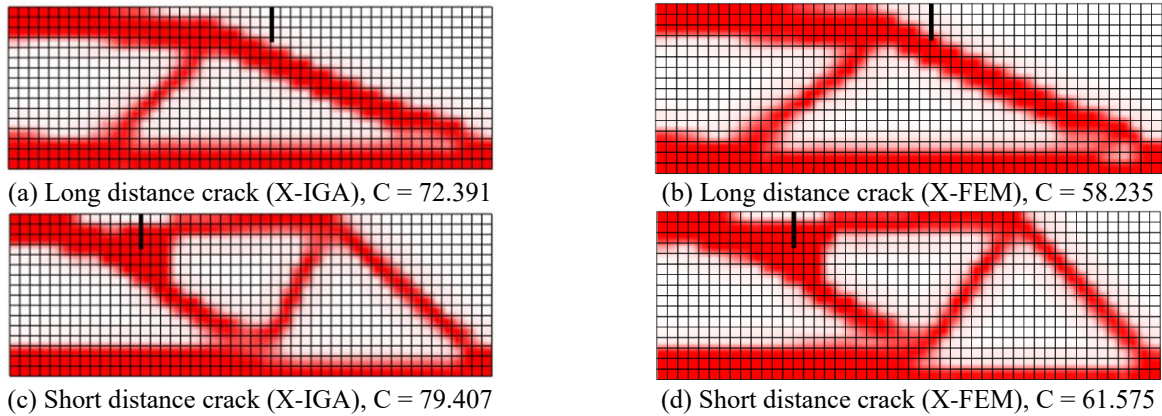


Fig. 16 Optimal single material topologies

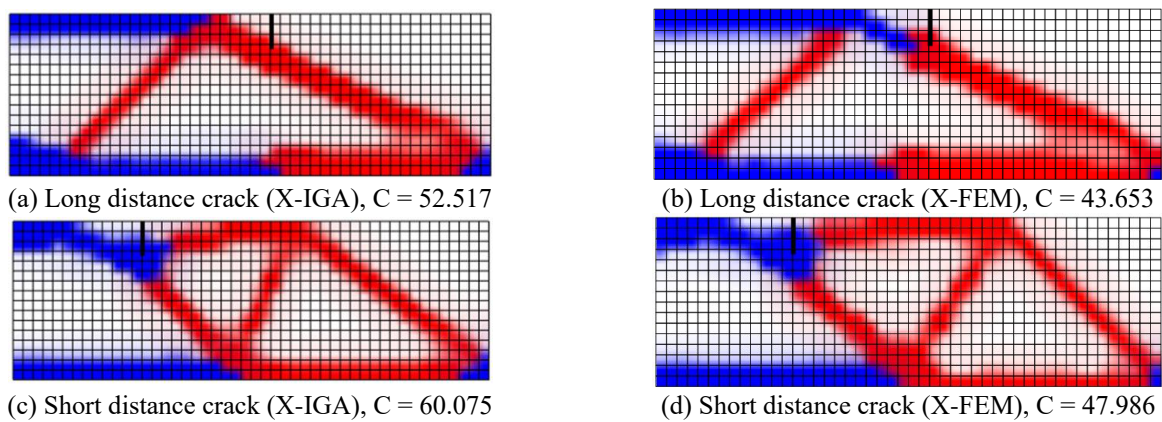


Fig. 17 Optimal two materials topologies

types used in the analysis, and \mathbf{F} is fixed. Therefore, lower bound solutions of the strain energy to its exact solution are obtained and indicated by Lieu and Lee (2017). In other words, topology optimization with X-IGA produces higher compliance converged values than with standard X-FEM but more accurate outcomes in terms of multi-material topology optimization than conventional X-FEM.

5.3 Optimal topology generation results under a mechanical description of Initial crack's angle

Crack angle (θ) cases of $45^\circ, 90^\circ, 135^\circ$ and 170° are considered as shown in Fig. 19 using the same crack with short distance $d = 6$ and long length $a = 4.125$.

Figs. 20 and 21 show optimized topology results considering single material and two materials using four types of crack's angle. As can be seen, the use of multiple materials may produce stiffer structures than a single material.

Fig. 22 describes convergence histories of objective functions. Converged compliance gradually increases when the angle changes from θ to 90° . The largest compliance value is 123.779 for a single material and 99.648 for two materials at the same angle $\theta = 90^\circ$. Moreover, assuming that $\bar{\theta} = \theta - 90^\circ$ with the same

magnitude $|\bar{\theta}|$, compliance values of $\bar{\theta} < 0$ are larger than those of $\bar{\theta} > 0$. It shows that compliance values of structure rely on the change of crack's angle.

6. Conclusions

This study proposes a novel numerical approach of multi-material optimal topology design based on eXtended IsoGeometric Analysis for crack problems. Several numerical examples are investigated for topologically optimal multi-material beam with variable crack information such as the length, distance, and angle. This study shows that eXtended IsoGeometric Analysis is also a suitable analysis model, which produces multi-material topology optimization robustness. The mechanical description of X-IGA evaluates a numerical interaction between cracks and multiple materials for topology optimization in comparisons with X-FEM. As a result, despite giving the higher values of compliances, the X-IGA method may contribute to more accurate outcomes in terms of topology optimization than X-FEM. Additionally, it is verified that optimal structures may retrofit a higher stiffness than single-material structures by using multiple materials.

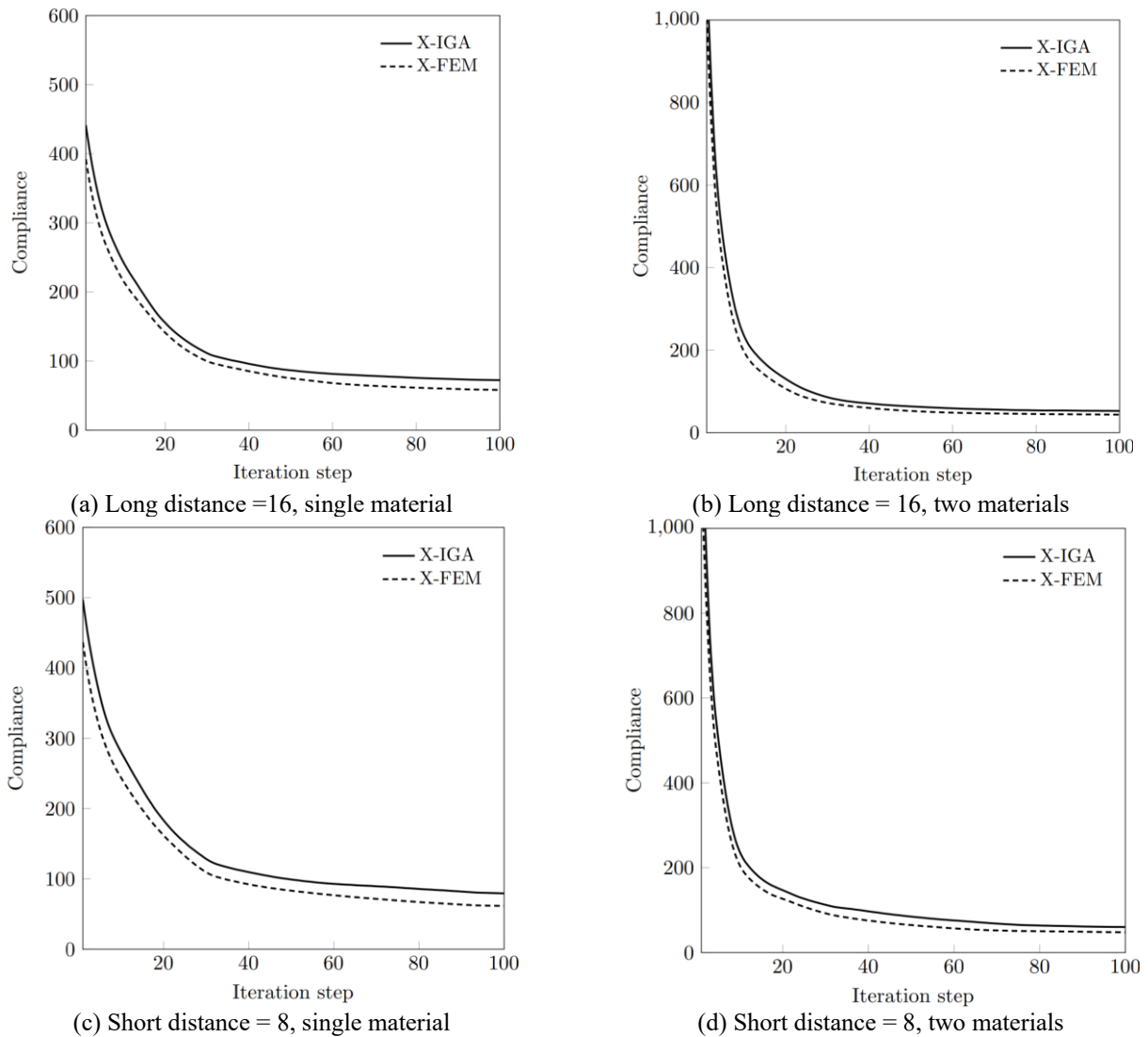


Fig. 18 Convergence histories of objective functions dealing with X-IGA and X-FEM in example 2

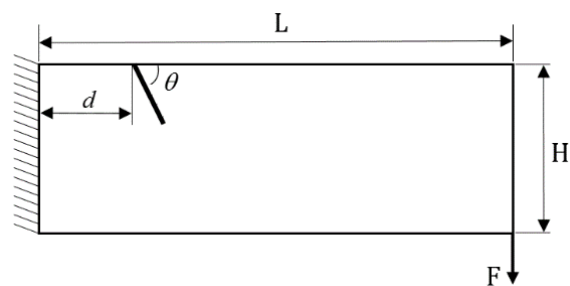


Fig. 19 Problem definition evaluating the influence of one crack angle in a given design domain

For the promising possibility of industrial application, topology optimization can improve 3-dimensional design models with constrained parameters to obtain optimized CAD models uploading it on a 3D printing system. Therefore, this paper gives intuitive and useful information to CAD designers for modeling of X-IGA, structural engineers for reinforcement by topology optimization, and manufacturers for multi-material products.

Acknowledgments

This research was supported by a grant (NRF-2020R1A4A2002855) from NRF (National Research Foundation of Korea) funded by MEST (Ministry of Education and Science Technology) of Korean government.

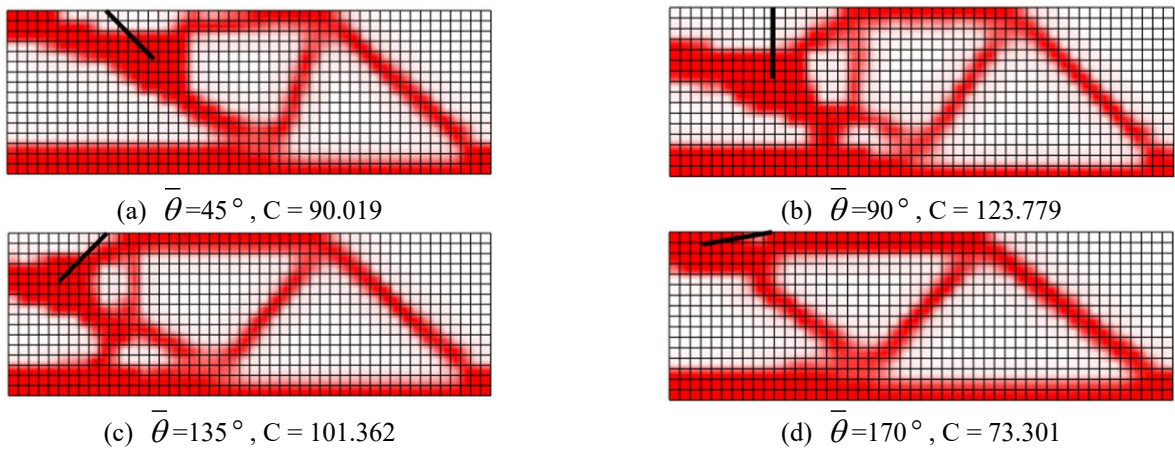


Fig. 20 Optimal single material topologies

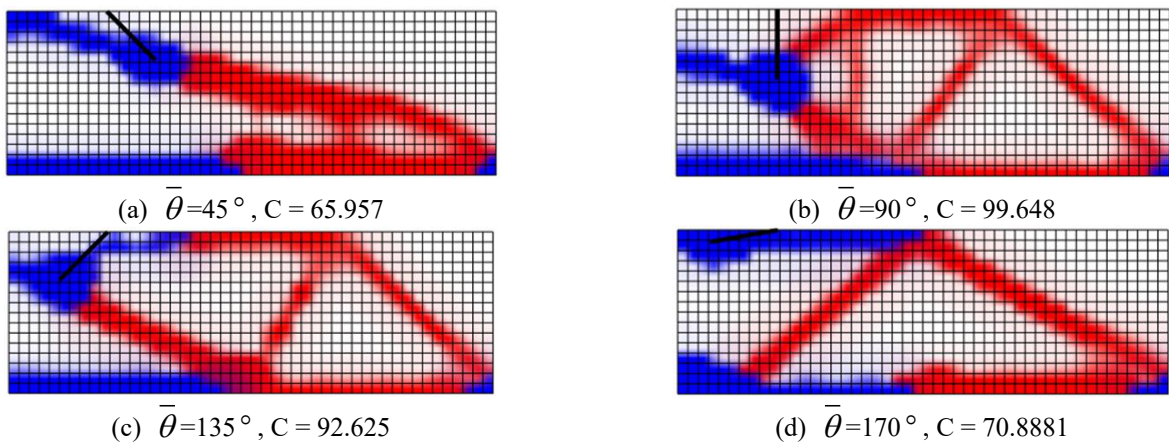
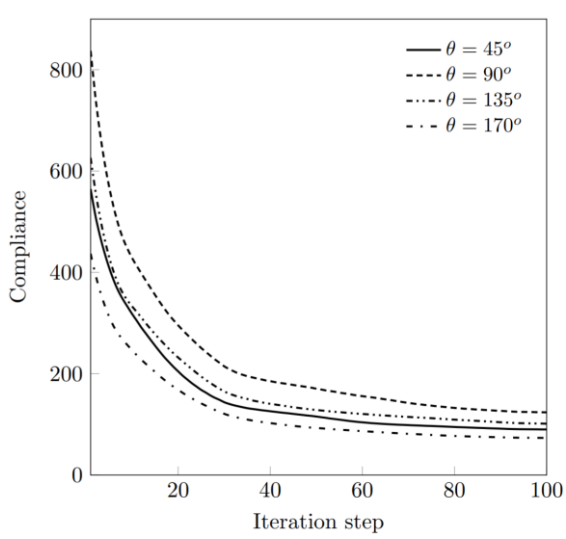
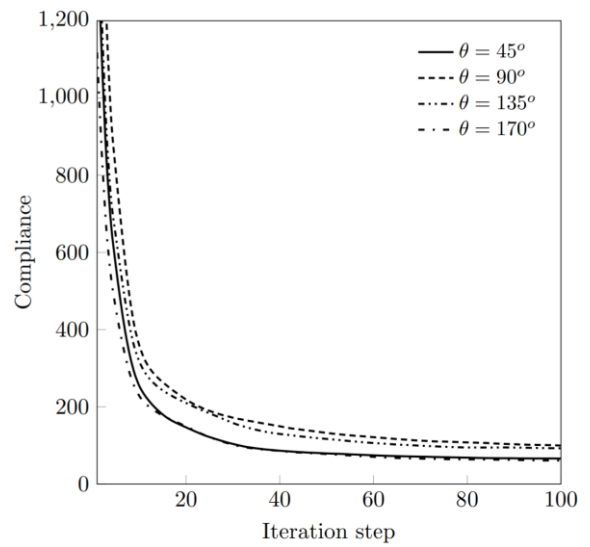


Fig. 21 Optimal two materials topologies



(a) Crack angle change and single material



(b) Crack angle change and two materials

Fig. 22 Convergence histories of objective function in example 3

References

- Alonso, C., Ansola, R. and Querin, O.M. (2014), "Topology synthesis of multi-material compliant mechanisms with a Sequential Element Rejection and Admission method", *Finite Elem. Anal. Des.*, **85**, 11-19. <https://doi.org/10.1016/j.finel.2013.11.006>.
- Banh, T.T. and Lee, D. (2018b), "Multi-material topology optimization of Reissner-Mindlin plates using MITC4", *Steel Compos. Struct.*, **27**(1), 27-33. <https://doi.org/10.12989/scs.2018.27.1.027>.
- Banh, T.T. and Lee, D. (2019), "Topology optimization of multi-directional variable thickness thin plate with multiple materials", *Struct. Multidiscip. O.*, **59**, 1503-1520. 10.1007/s00158-018-2143-8.
- Banh, T.T. and Lee, DK (2018a), "Multi-material topology optimization design for continuum structures with crack patterns", *Compos. Struct.*, **186**, 193-209. 10.1016/j.compstruct.2017.11.088.
- Bendsoe, M.P. and Kikuchi, N. (1988), "Generating optimal topologies in structural design using a homogenization method", *Comput. Method. Appl. M.*, **71**(2), 197-224. [https://doi.org/10.1016/0045-7825\(88\)90086-2](https://doi.org/10.1016/0045-7825(88)90086-2).
- Benson, D.J., Bazilevs, Y., Luycker, E.D. and Belytschko, T. (2010), "A generalized finite element formulation for arbitrary basis functions: From isogeometric analysis to XFEM", *Int. J. Numer. Method. Eng.*, **83**, 765-785. <https://doi.org/10.1002/nme.2864>.
- Buffa, A., Sangalli, G. and Vazquez, R. (2010), "Isogeometric analysis in electromagnetics: B-splines approximation", *Comput. Method. Appl. M.*, **199**, 17-20. <https://doi.org/10.1016/j.cma.2009.12.002>.
- Cottrell, J.A., Hughes, T.J.R. and Bazilevs, Y. (2009), *Isogeometric Analysis: Toward Integration of CAD and FEA*, John Wiley and Sons, United Kingdom.
- Doan, Q.H. and Lee, D. (2019), "Optimal formation assessment of multi-layered ground retrofit with arch-grid units considering buckling load factor", *Int. J. Steel Struct.*, **19**, 269-282. <https://doi.org/10.1007/s13296-018-0115-x>.
- Ghorashi, S.S., Valizadeh, N. and Mohammadi, S. (2012), "Extended isogeometric analysis for simulation of stationary and propagating cracks", *Int. J. Numer. Method. Eng.*, **89**, 1069-1101. 10.1002/nme.3277.
- Hughes, T.J.R., Cottrell, J.A. and Bazilevs, Y. (2005), "Isogeometric analysis: CAD, finite elements, NURBS, exact geometry and mesh refinement", *Comput. Method. Appl. M.*, **194**, 4135-4195. <https://doi.org/10.1016/j.cma.2004.10.008>.
- Khatir, S. and Abdek Wahab, M. (2018), "Fast simulations for solving fracture mechanics inverse problems using POD-RBF XIGA and Jaya algorithm", *Eng. Fract. Mech.*, doi:10.1016/j.engfracmech.2018.09.032.
- Khatir, S. and Abdek Wahab, M. (2019), "A computational approach for crack identification in plate structures using XFEM, XIGA, PSO and Jaya algorithm", *Theor. Appl. Fract. Mech.*, **103**, 102240. <https://doi.org/10.1016/j.tafmec.2019.102240>.
- Khatir, S., Benaissa, B., Roberto, C. and Abdek Wahab, M. (2017), "Damage detection in CFRP composite beams based on vibration analysis using proper orthogonal decomposition method with radial basis function and Cuckoo Search algorithm", *Compos. Struct.*, **187**, 344-353. <https://doi.org/10.1016/j.compstruct.2017.12.058>.
- Khatir, S., Boutchicha, D., Le, C.T., Tran, H.N., Nguyen, T.N. and Abdek Wahab, M. (2020), "Improved ANN technique combined with Jaya algorithm for crack identification in plates using XIGA and experimental analysis", *Theor. Appl. Fract. Mech.*, **107**, 102554. <https://doi.org/10.1016/j.tafmec.2020.102554>.
- Khatir, S., Tiachacht, S., Cuong-LeThanh, Quoc Bui T. and Abdel Wahab, M. (2019a), "Damage assessment in composite laminates using ANN-PSO-IGA and Cornwell indicator", *Compos. Struct.*, **230**, 111509. <https://doi.org/10.1016/j.compstruct.2019.111509>.
- Khatir, S., Wahab, M.A., Djilali, B. and Khatir, T. (2019b), "Structural health monitoring using modal strain energy damage indicator coupled with teaching-learning-based optimization algorithm and isogeometric analysis", *J. Sound Vib.*, **448**, 230-246. <https://doi.org/10.1016/j.jsv.2019.02.017>.
- Lee, D., Starossek, U. and Shin, S. (2010), "Topological optimized design considering dynamic problem with non-stochastic structural uncertainty", *Struct. Eng. Mech.*, **36**(1), 79-94. <https://doi.org/10.12989/sem.2010.36.1.079>.
- Lieu, Q.X. and Lee, J. (2017), "Multiresolution topology optimization using isogeometric analysis", *Int. J. Numer. Method. Eng.*, **114**, 2025-2047. 10.1002/nme.5593.
- Liu, Q., Chan, R. and Huang, X. (2016), "Concurrent topology optimization of macrostructures and material microstructures for natural frequency", *Mater. Design*, **106**, 380-390. <https://doi.org/10.1016/j.matdes.2016.05.115>.
- Moes, N., Dolbow, J. and Belytschko, T. (1999), "A Finite Element Method for Crack Growth without Remeshing", *Int. J. Numer. Method. Eng.*, **46**, 131-150. [https://doi.org/10.1002/\(SICI\)10970207\(19990910\)46:1<131::AID-NME726>3.0.CO;2-J](https://doi.org/10.1002/(SICI)10970207(19990910)46:1<131::AID-NME726>3.0.CO;2-J).
- Mohammadi, S. (2008), *Extended Finite Element Method: for Fracture Analysis of Structures*, Blackwell Publishing Ltd, United Kingdom.
- Nazargah, M.L. (2014), "An isogeometric approach for the analysis of composite steel-concrete beams", *Eng. Fract. Mech.*, **84**, 406-415. <https://doi.org/10.1016/j.tws.2014.07.014>.
- Nguyen, A.P., Banh, T.T., Lee, DK, Lee, J., Kang, J., Shin, S. (2018), "Design of multiphase carbon fiber reinforcement of crack existing concrete structures using topology optimization", *Steel Compos. Struct.*, **29**(5), 635-645. <https://doi.org/10.12989/scs.2018.29.5.635>.
- Nguyen, V.P. and Bordas, S. (2005), "Extended Isogeometric Analysis for Strong and Weak Discontinuities", *Isogeometric Method. Numer. Simul.*, 21-120. https://doi.org/10.1007/978-3-7091-1843-6_2.
- Qian, X. (2010), "Full analytical sensitivities in NURBS based isogeometric shape optimization", *Comput. Method. Appl. M.*, **199**, 29-32. <https://doi.org/10.1016/j.cma.2010.03.005>.
- Qian, X. (2013), "Topology optimization in B-spline space", *Comput. Method. Appl. M.*, **265**, 15-35. 10.1016/j.cma.2013.06.001.
- Qiao, S., Han, X., Zhou, K. and Ji, J. (2016), "Seismic analysis of steel structure with brace configuration using topology optimization", *Steel Compos. Struct.*, **21**(3), 501-515. <https://doi.org/10.12989/scs.2016.21.3.501>.
- Shobeiri, V. (2015), "The topology optimization design for cracked structures", *Eng. Anal. Bound. Elem.*, **58**, 26-38. 10.1016/j.enganbound.2015.03.002.
- Shojaee, S. and Daneshmand, A. (2015), "Crack analysis in media with orthotropic Functionally Graded Materials using eXtended Isogeometric Analysis", *Eng. Fract. Mech.*, **147**, 203-227. 10.1016/j.engfracmech.2015.08.025.
- Tavakoli, R. and Mohsenind, S.M. (2014), "Alternating active-phase algorithm for multimaterial topology optimization problems: a 115-line MATLAB implementation", *Struct. Multidiscip. O.*, **49**, 621-642. 10.1007/s00158-013-0999-1.
- Wall, W.A., Frenzel, M.A. and Cyron, C. (2008), "Isogeometric structural shape optimization", *Comput. Method. Appl. M.*, **197**, 2976-2988. <https://doi.org/10.1016/j.cma.2008.01.025>.
- Yang, Z., Zhou, K. and Qiao, S. (2018), "Topology optimization

- of reinforced concrete structure using composite truss-like model”, *Struct. Eng. Mech.*, **67**(1), 79-85. <https://doi.org/10.12989/sem.2018.67.1.079>.
- Yi, L.V. and Liu, S. (2018), “Topology optimization and heat dissipation performance analysis of a micro-channel heat sink”, *Meccanica*, **53**, 3693-3708. 10.1007/s11012-018-0918-z.
- Yun, K.S. and Youn, S.K. (2017), “Multi-material topology optimization of viscoelastically damped structures under time-dependent loading”, *Finite Elem. Anal. Des.*, **123**, 9-18. 10.1016/j.finel.2016.09.006.
- Zhou, S. and Wang, M.Y. (2007), “Multimaterial structural topology optimization with a generalized Cahn–Hilliard model of multiphase transition”, *Struct. Multidiscip. O.*, **33**, 89-111. 10.1007/s00158-006-0035-9.
- Zhou, S.W. and Wang, M.Y. (2006a), “Multimaterial structural topology optimization with a generalized Cahn–Hilliard model of multiphase transition”, *Struct. Multidiscip. O.*, **33**, 89-111. 10.1007/s00158-006-0035-9.
- Zhou, S.W. and Wang, M.Y. (2006b), “3D Multi-material structural topology optimization with the generalized Cahn–Hilliard equations”, *Comput. Model. Eng. Sci.*, **16**, 83-101. <http://hdl.handle.net/1783.1/74250>.
- Zuo, K.T., Chen, L.P., Zhang, Y.Q. and Yang, J. (2007), “Study of key algorithms in topology optimization”, *Int. J. Adv. Manufact. Technol.*, **32**, 787-796. 10.1007/s00170-005-0387-0.